LLNL-PROC-531854

LAWRENCE
LIVERMORE
NATIONAL
LABORATORY

Photon Strength and the Low-Energy Enhancement

M. Wiedeking, L. A. Bernstein, M. Krticka, D. L. Bleuel, J. M. Allmond, M. S. Basunia, J. T. Burke, P. Fallon, R. B. Firestone, B. L. Goldblum, R. Hatarik, P. T. Lake, I. Y. Lee, S. R. Lesher, S. Paschalis, M. Petri, L. Phair, N. D. Scielzo

February 23, 2012

Frontiers in Gamma-Ray Spectroscopy 2012 - FIG12
New Delhi, Iceland
March 5, 2012 through March 7, 2012

Photon strenght and the low-energy enhancement

M. Wiedeking,[1, 2, *] L. A. Bernstein,[1] M. Krtička,[3] D. L. Bleuel,[1] J. M. Allmond,[4, †]
M. S. Basunia,[5] J. T. Burke,[1] P. Fallon,[5] R. B. Firestone,[5] B. L. Goldblum,[5, 6, 7] R. Hatarik,[1]
P. T. Lake,[5] I-Y. Lee,[5] S. R. Lesher,[1] S. Paschalis,[5] M. Petri,[5] L. Phair,[5] and N. D. Scielzo[1]

[1] *Physical and Life Sciences Directorate, Lawrence Livermore National Laboratory, Livermore, California 94551, USA*
[2] *iThemba LABS, P.O. Box 722, Somerset West 7129, South Africa*
[3] *Faculty of Mathematics and Physics, Charles University, V Holešovičkách 2, Prague 8, Czech Republic*
[4] *Department of Physics, University of Richmond, Virginia 23173, USA*
[5] *Nuclear Science Division, Lawrence Berkeley National Laboratory, Berkeley, California 94720, USA*
[6] *Department of Nuclear Engineering, University of California, Berkeley, California 94720, USA*
[7] *Department of Nuclear Engineering, University of Tennessee, Knoxville, Tennessee 37996, USA*

I. INTRODUCTION

The ability of atomic nuclei to emit and absorb photons with energy E_γ is known as the photon strength function $f(E_\gamma)$. It has direct relevance to astrophysical element formation via neutron capture processes [1, 2] due to its central role in nuclear reactions. Studies of $f(E_\gamma)$ have benefited from a wealth of data collected in neutron capture [3] and direct reactions [4] but also from newly commissioned inelastic photon scattering facilities [5, 6]. The majority of these experimental methods, however, rely on the use of models because measured γ-ray spectra are simultaneously sensitive to both the nuclear level density and $f(E_\gamma)$.

As excitation energy increases towards the particle separation energies, the level density increases rapidly, creating the quasi-continuum. Nuclear properties in this excitation energy region are best characterized using statistical quantities, such as $f(E_\gamma)$. A point of contention in studies of the quasi-continuum has been an unexpected and unexplained increase in $f(E_\gamma)$ at low γ-ray energies (i.e. below $E_\gamma \approx 3$ MeV) in a subset of light-to-medium mass nuclei [7–12]. Ideally, a new model-independent experimental technique is required to address questions regarding the existence and origin of this low-energy enhancement in $f(E_\gamma)$.

Here such a model-independent approach is presented for determining the shape of $f(E_\gamma)$ over a wide range of energies. The method involves the use of coupled high-resolution particle and γ-ray spectroscopy to determine the emission of γ rays from the quasi-continuum in a nucleus with defined excitation energy to individual discrete levels of known spins and parities. This method shares characteristics of two neutron capture-based techniques: the Average Resonance Capture (ARC) [13, 14] and the Two-Step Cascade analysis (TSC) [15]. The power of the new technique lies in the additional ability to positively identify primary γ-ray decay from defined excitation energy regions to low-lying discrete states. This approach was used to study the shape of $f(E_\gamma)$ in ^{95}Mo populated in the (d,p) direct reaction.

II. EXPERIMENTAL METHOD

The measurement was carried out at the 88-Inch Cyclotron of the Lawrence Berkeley National Laboratory. ^{95}Mo nuclei were produced by the ^{94}Mo(d,p-2γ) reaction at a beam energy of 11 MeV and a target thickness of 250(6) μg/cm^2. The average beam current during the 3-day experiment was $\sim$5.5 nA. The STARS-LIBERACE detector array [16], consisting of Compton suppressed HPGe Clover-type detectors [17, 18] and large-area segmented annular silicon detectors (ΔE-E telescope) of the S2 type [19], was used to detect coincident γ radiation and charged particles. Five Clover detectors were placed at a distance of 20 cm from the center of the target chamber. Two identical particle telescopes were placed on opposite sides of the target with 150 μm ΔE and 1000 μm E detectors. The telescopes were mounted 2.1 cm and 1.6 cm from the target for the downstream and upstream particle telescopes covering an angular range of 28° to 56° and 118° to 145°, respectively.

A valid particle trigger required detection of charged particles in the one of the two telescopes within a coincidence interval of $\sim$400 ns. An event was recorded when the particle coincidence condition and an γ-ray event of multiplicity one or greater were correlated within a 550 ns time window which was reduced to 100 ns in the offline analysis.

In-beam resolutions of $\sim$200 keV FWHM were measured for the particle telescopes from directly populated states. Germanium detector energy and efficiency calibrations were performed using a standard ^{152}Eu γ-ray source. The 204 keV transition from the first-excited state in ^{95}Mo is of particular importance to this work. With the efficiency curve exhibiting rapid changes between the values determined by the 121 and 344 keV ^{152}Eu transitions, the efficiency for the 204 keV transition was determined separately from particle-γ and particle-γ-γ coincidence data and is 2.4(1)%. The

*corresponding author: wiedeking@tlabs.ac.za; Permanent address: iThemba LABS, P.O. Box 722, Somerset West 7129, South Africa
†Current address: Oak Ridge National Laboratory, Oak Ridge, Tennessee 37831, USA

medium and high-energy γ-ray efficiency was determined using ^{12}C(d,p)^{13}C and ^{13}C(d,p)^{14}C reactions. The γ-ray photo-peak detection efficiency in add-back mode for a 1 MeV transition is 1.03(4)%, decreases to 0.53(4)% for the 3.09 MeV ^{13}C γ-ray, and to 0.26(3)% for the 6.90 MeV ^{14}C line. These efficiencies for high-energy γ-ray transitions are comparable to those reported for the AFRODITE array [20] comprised of the same Clover detectors in a similar configuration.

The experiment was designed to investigate statistical feeding from the quasi-continuum to individual low-lying discrete levels (EL_j) in ^{95}Mo. A key aspect is the detection and extraction of correlated particle-γ-γ events. Proton energies from the silicon telescopes determine the entrance excitation energy (E$_i$) into the residual nucleus produced in the reaction. Tagging on γ-ray transitions originating from low-lying discrete levels specifies the states which are being fed by the primary γ rays (E$_\gamma$). When a discrete transition E$_{L_j}$ is detected in coincidence with a proton, additional requirements are applied to the second γ ray, E$_\gamma$, so that the energy sum of E$_{L_j}$ and E$_\gamma$ be equal to E$_i$ $\pm$ 200 keV. Any particle-γ-γ event satisfying these conditions provides an unambiguous determination of the origin and destination of the observed primary transition. The feeding to individual levels is extracted on an event-by-event basis and each observed transition is efficiency corrected for the primary and discrete γ-ray energies. Fig. 1 illustrates this procedure.

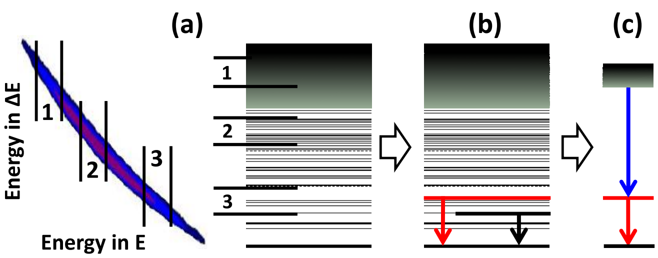

FIG. 1: Step-by-step procedure to extract primary γ transitions to individual discrete levels. (a) Tagging on different proton energies determines the entrance excitation energy of the nucleus populated in the reaction. High (low) proton energies yield low (high) excitation energies. (b) The discrete levels are selected by tagging on γ rays emitted from these states. (c) Applying the energy sum condition of discrete and primary γ-ray energies be equivalent to the excitation energy (e.g. 1) provides events of unambiguous origin and destination.

III. RESULTS

The γ-ray strength of the primary decay between the gated quasi-continuum region E_i and discrete level with energy E_{Lj} is extracted according to the expression [21]

$$f(E_\gamma) \equiv f_{J^\pi}(E_\gamma) = \frac{\overline{\Gamma}_{J^\pi}(E_i, E_\gamma)\rho_{J^\pi}(E_i)}{E_\gamma^{2\lambda+1}} \qquad (1)$$

where $\overline{\Gamma}_{J^\pi}(E_i, E_\gamma)$ is the average width of primary γ rays with energy E_γ from excitation enegy E_i, $\rho_{J^\pi}(E_i)$ is the level density at E_i, and λ is the multipolarity of the transition. The first equivalence is based on the Brink hypothesis [22].

$\overline{\Gamma}_{J^\pi}(E_i, E_\gamma)$ can be related to the number of primary γ-ray events $N_{L_j}(E_i)$ detected which are corrected for the total decay intensity of the discrete level, for the efficiencies to detect the discrete γ ray and the primary γ transition. The model-dependent level density term $\rho_{J^\pi}(E_i)$ in Eq.(1) as well as systematic uncertainties can be eliminated by taking the ratio R of $f(E_\gamma)$ for two different primary γ-ray energies from the same initial excitation energy E_i to discrete low-lying levels of same spin and parity at energies E_{L_1} and E_{L_2} as

$$R = \frac{f(E_i - E_{L_1})}{f(E_i - E_{L_2})} = \frac{N_{L_1}(E_i)(E_i - E_{L_2})^3}{N_{L_2}(E_i)(E_i - E_{L_1})^3} \qquad (2)$$

With the energy sum, particle, and γ-ray tagging requirements, this work focuses on a very specific branch of primary de-excitation. None of the target contaminants, ^{16}O and ^{12}C, interfere when extracting primary decays to discrete levels due to these tagging specifications. The ratios are obtained entirely from experimentally-measured quantities and are free of model dependencies.

In this work a total of 24 ratios were obtained using seven $3/2^+$ and two each for the $1/2^+$, $7/2^+$, and $9/2^+$ discrete states, all below 1.7 MeV excitation energy with one exception at 3.04 MeV. Table 1 summarizes the properties of the discrete levels which are used to determine the ratios.

Only levels observed in previous studies [23] and verified in the present work using proton-γ and proton-γ-γ coincidence events [24] were used. Published level and transition energies as well as spin assignments [23], are generally in agreement; just three minor discrepancies were identified. For the 1370 keV level, the $3/2^+$ assignment was reported in an early (d,p) measurement [25], in agreement with current results. The positive-parity character was verified in a ($\vec{p}$,d) reaction [26]. The level at 1426 keV has been reported as $3/2^+$ [25, 26], in agreement with a 3/2 spin assignment from the present analysis. The level at 1660 keV exhibits spin 3/2 characteristics, consistent with $\leq 5/2$ [23]. For this state the assumption of positive parity is made.

Fig. 2 shows four sample ratios from this work denoted as $R_{(d,p)} = f_{(d,p)}(E_i - E_{L_1})/f_{(d,p)}(E_i - E_{L_2})$ (solid line). The $R_{(d,p)}$ results are compared to $(^3He, \alpha)$ data (dotted line in Fig. 2) from the CACTUS array [8], which were analyzed using the Oslo Method [27] and are labelled as $R_{(^3He,\alpha)} = f_{(^3He,\alpha)}(E_i - E_{L_1})/f_{(^3He,\alpha)}(E_i - E_{L_2})$. To facilitate the comparison, the $(^3He, \alpha)$ data were fitted using a quadratic polynomial in the γ-ray energy range of 1 to 6.5 MeV, as shown in Fig. 3. A polynomial was also fitted to the upper and lower uncertainties.

TABLE I: Discrete levels used to extract the number of primary γ-ray events $N_{L_j}(E_i)$.E_{L_j} is the excitation energy of the discrete level, J^π indicates its spin and parity. E_{L_γ} is the γ-ray transition used in coincidence with the primary transitions (if two transitions are listed then both are used to extract the strength), BR is the measured branching ratio normalized to the strongest transition originating from each discrete level and I_{tot} is the total decay intensity from each of the discrete levels E_{L_j} (the strongest transition corresponds to 1).

E_{L_j} (keV)	J^π	E_{L_γ} (keV)	BR (%)	I_{tot}
204	$3/2^+$	204	100	1
821	$3/2^+$	821	100	1.27(4)
		616	27(4)	1.27(4)
1370	$3/2^+$	1370	100	1.48(8)
		1166	48(8)	1.48(8)
1426	$3/2^+$	1222	100	1.32(5)
1620	$3/2^+$	1620	100	1.28(3)
1660	$3/2^+$	1457	100	1
3043	$3/2^+$	3043	100	2.12(7)
786	$1/2^+$	582	100	1.3(5)
		786	30(5)	1.3(5)
1039	$1/2^+$	835	100	1.15(2)
766	$7/2^+$	766	100	1
1074	$7/2^+$	1074	100	1.17(10)
948	$9/2^+$	948	100	1
1552	$9/2^+$	604	100	1.6(8)

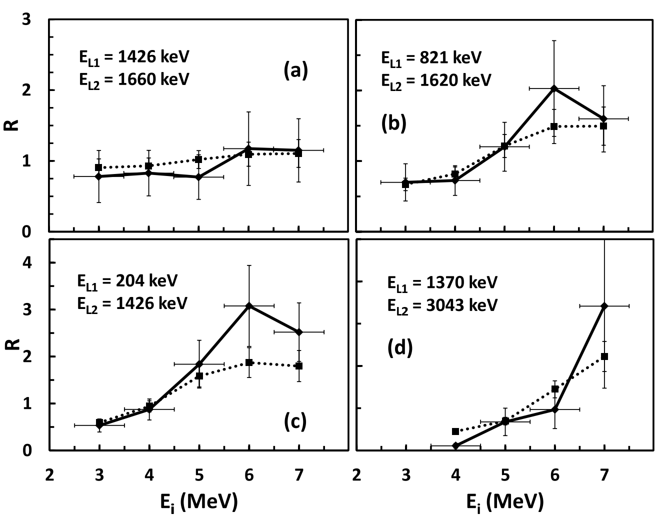

FIG. 2: The ratio $R_{(d,p)} = f_{(d,p)}(E_i - E_{L1})/f_{(d,p)}(E_i - E_{L2})$ as a function of excitation energy E_i from this work using the (d,p) reaction (solid lines). E_{L1} and E_{L2} shown in each panel indicate the low-lying discrete levels (all $3/2^+$ in this figure) being fed by the primary transitions. For each ratio the numerator includes the higher-energy primary transition (lower discrete energy state). The ratios are plotted in terms of excitation energy and the horizontal error bars are representative of the bin size. Dotted lines are ratios $R_{(^3He,\alpha)} = f_{(^3He,\alpha)}(E_i - E_{L1})/f_{(^3He,\alpha)}(E_i - E_{L2})$ extracted from $(^3He,\alpha)$ data by Guttormsen *et al.* [8].

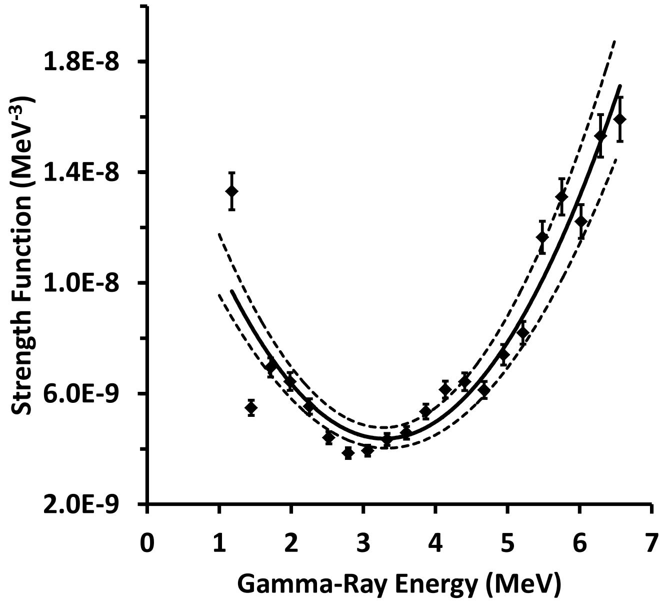

FIG. 3: Quadratic polynomial fits (solid line) to the $(^3He,\alpha)$ data (filled points) [8]. The upper and lower error bars, fitted as discussed in the text, are shown by dashed curves.

IV. DISCUSSION

For consistency the strength to the higher-energy discrete level E_{L_2} (lower primary γ-ray energy) is found in the denominator of all ratios in Fig. 2. When the energies of the primary decays in a ratio are similar (i.e. decay to discrete levels E_{L_1} and E_{L_2} of similar energy as shown in fig. 2(a)). $R_{(d,p)}$ does not exhibit much variation and has a value of ~1 across all excitation energies. Although expected, this result serves as an important consistency check and adds confidence in the detector efficiency calibrations and spin assignments.

The observed drop in the ratios (fig. 2(b), (c), and (d)) with decreasing excitation energy are correlated with the increase in primary γ-ray energy spread between the numerator and denominator. The largest energy spread is found from the E_{L_2}=3043 keV level and a rapid decrease towards lower excitation energies is observed (fig. 2(d)). At intermediate energy differences (fig. 2(b) and (c)) the decrease is clearly visible but less dramatic. Generally, $f_{(d,p)}(E_i - E_{L_1})$ is larger at higher excitation energies for the higher-energy primary transitions (in the numerator) compared to $f_{(d,p)}(E_i - E_{L_2})$ with the lower primary γ ray (denominator). At lower excitation energies (< 3 - 4 MeV) the statement is reversed. Similar statements can be made for all 24 ratios form this work. Large uncertainties, in particular at high excitation energies, are mostly due to limited statistics.

Ratios $R_{(d,p)}$ are compared to the ratios $R_{(^3He,\alpha)}$ determined from the polynomial curve fitted to the data by Guttormsen *et al.* [8] shown in Fig. 3. The ratios from the present study are given in terms of excitation energy while the $(^3He,\alpha)$ data are in terms of γ-ray energy and a conversion is necessary, as illustrated in an example with primary transitions originating from E_i=6 MeV excitation energy. The energy of the primary transition feeding the E_{L_1}=204 keV level is 5796 keV and 4340 keV for transitions feeding the E_{L_2}=1660 keV level. It is these primary γ-ray energies and their associated strength from which the ratio is obtained from the $(^3He,\alpha)^{95}$Mo results and compared to the result of the 6 MeV excitation energy ratio of the (d,p)^{95}Mo data. Ratios $R_{(^3He,\alpha)}$ obtained in this way are shown as data points connected by dotted curves in Fig 2. Overall, $R_{(d,p)}$ compares very well to $R_{(^3He,\alpha)}$.

Instead of discussing 24 individual ratios the comparison between the two data sets is facilitated using residuals, shown in Fig. 4, and defined as

$$\delta = \frac{R_{(3He,\alpha)} - R_{(d,p)}}{\sqrt{\sigma^2_{(3He,\alpha)} + \sigma^2_{(d,p)}}} \tag{3}$$

Positive (negative) δ indicate that the ratio value of $f_{(d,p)}(E_\gamma)$ decreases (increases) more rapidly compared to $f_{(3He,\alpha)}(E_\gamma)$. The deviations ($\delta < 0$) at $E_i = 6$ and 7 MeV indicate that $f_{(d,p)}(E_\gamma)$ is somewhat steeper than $f_{(3He,\alpha)}(E_\gamma)$ for $E_\gamma \gtrsim 5$ MeV. At $E_i = 4$ MeV six values (some of them overlap) are found with $\delta > 1.5$ and are due to ratios with E_{L_2}=3043 keV suggesting an even larger enhancement in $f_{(d,p)}(E_\gamma)$ compared to $f_{(3He,\alpha)}(E_\gamma)$. Of course, not all δ values corresponding to a specific E_i and J^π are independent.

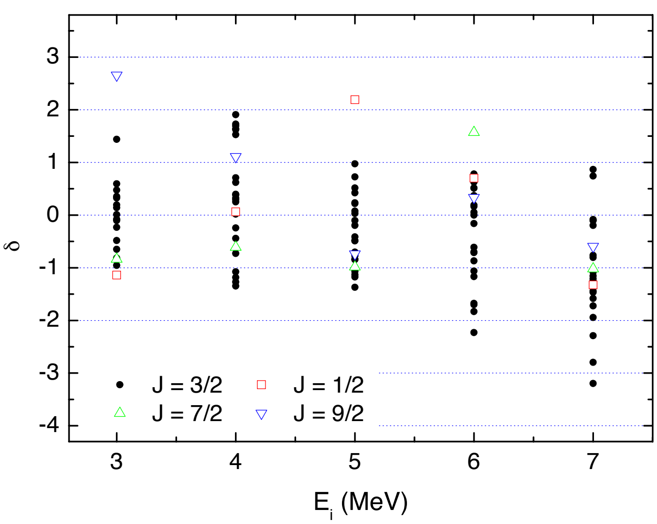

FIG. 4: (Color online) Differences between $R_{(d,p)} = f_{(d,p)}(E_i - E_{L_1})/f_{(d,p)}(E_i - E_{L_2})$ and $R_{(3He,\alpha)} = f_{(3He,\alpha)}(E_i - E_{L_1})/f_{(3He,\alpha)}(E_i - E_{L_2})$ deduced from the fit to previous data [8] expressed in terms of residual δ. Ratios with the 3043 keV level do not contribute to the 3 MeV excitation-energy region.

The good agreement between present and previous data confirms the shape of the photon strength function as reported by Guttormsen *et al.* [8]. It should be noted that the present measurement examines photon strength to individual discrete levels only, while the previous work [8] determined the total strength without specific requirements on the energy of the level that is fed by the primary transitions. Due to the gating and energy sum requirements this work allows for determination of the origin of the low-energy enhancement which has so far eluded measurements. The observed increase in $f(E_\gamma)$ is due to transitions originating from relatively low excitation energies, $E_x < 5MeV$. However, this study specifically examines only these excitation and γ-ray energies and no statement can be made regarding the possibility of the low-energy primary transitions from higher-excitation energy regions also displaying an enhancement. This is due to the lack of a strongly populated discrete state with $E_x \gg$ 3 MeV. Any conclusions regarding the regions of higher-excitation energies can only be made by invoking the Brink Hypothesis.

The present work clearly supports the picture of an $f(E_\gamma)$ increase at low-energies in ^{95}Mo but more measurements are desirable. An experimental campaign populating the same residual nucleus in different reactions may provide valuable insight into the enhancement and its physical origin. With the enhancement only observed in light and medium mass nuclei, it will also be very interesting to use this new technique in studies on heavier nuclei.

V. SUMMARY

A new experimental technique to extract the relative photon strength from the quasi-continuum to known individual discrete levels has been presented. This approach is free of model dependencies and ^{95}Mo ratio values obtained in this work have been compared to data by Guttormsen *et al.* [8]. The good agreement confirms the minimum and low-energy enhancement in the photon strength function. The application of stringent gating requirements allows for the determination of the origin of the observed enhancement to be from the region of low-excitation energies. Further work using this new technique is desirable particularly in other mass regions.

VI. ACKNOWLEDGMENTS

The authors thank the operations staff at the 88-Inch Cyclotron of Lawrence Berkeley National Laboratory for a smooth run. This work is performed under the auspices of the U.S. Department of Energy Lawrence Livermore National Laboratory under contract DE-AC52-07NA27344 and University of Richmond under DE-FG52-06NA26206 and DE-FG02-05ER41379. For Lawrence Berkeley National Laboratory this work was supported by the Director, Office of Science, Office of Nuclear Physics, of the U.S. Department of Energy under Contract No. DE-AC02-05CH11231. MW acknowledges support from the National Research Foundation of South

Africa and MK from the research plan MSM 0021620859 of the Ministry of Education of the Czech Republic.

[1] C. Sneden, J. J. Cowan, and R. Gallino, Annual Review of Astronomy and Astrophysics 46, 241 (2008).
[2] G. J. Mathews and R. A. Ward, Rep. Prog. Phys. 48 1371 (1985).
[3] ND 2007 - International Conference on Nuclear Data for Science and Technology, Nice, France, April 22-27 2007, ISBN:978-2-7598-0090-2.
[4] N.K. Glendenning, *Direct Nuclear Reactions* (World Scientific Publishing Co. Pte. Ltd., 2004).
[5] H.R. Weller, *et al.*, Progress in Particle and Nuclear Physics 62, 257 (2009).
[6] R. Schwengner, *et al.*, Nucl. Instrum. Methods A 555, 211 (2005).
[7] A. Voinov *et al.*, Phys. Rev. Lett. **93**, 142504 (2004).
[8] M. Guttormsen *et al.*, Phys. Rev. C **71**, 044307 (2005).
[9] A.C. Larsen *et al.*, Phys. Rev. C **73**, 064301 (2006).
[10] A.C. Larsen *et al.*, Phys. Rev. C **76**, 044303 (2007).
[11] E. Algin *et al.*, Phys. Rev. C **78**, 054321 (2008).
[12] N.U.H. Syed *et al.*, Phys. Rev. C **80**, 044309 (2009).
[13] L.M. Bollinger and G. E. Thomas, Phys. Rev. C **2**, 1951 (1970).
[14] M.L. Stelts and J.C. Browne, Nucl. Instrum. Methods **55**, 253 (1978).
[15] F. Bečvař, *et al.*, Phys. Rev. C **46**, 1276 (1992).
[16] S.R. Lesher, *et al.*, Nucl. Instr. and Meth. A, (2010).
[17] G. Duchêne, *et al.*, Nucl. Instr. and Meth. A 432, 90 (1999).
[18] Z. Elekes, *et al.*, Nucl. Inst. and Meth. in Phys. Res. A **503**, 580 (2003).
[19] http://www.micronsemiconductor.co.uk
[20] M. Lipoglavšek, *et al.*, Nucl. Inst. and Meth. in Phys. Res. A **557**, 523 (2006).
[21] G.A. Bartholomew *et al.*, Adv. Nucl. Phys. **7**, 229 (1973).
[22] D.M. Brink, Ph.D. thesis, Oxford University, 1955.
[23] S.K. Basu, *et al.*, Nuclear Data Sheets 111, 2555 (2010).
[24] M. Wiedeking, *et al.*, manuscript in preparation.
[25] J.B. Moorhead and R.A. Moyer, Phys. Rev. **184**, 1205 (1969).
[26] S.A. Sultana, *et al.*, Phys. Rev. C **70**, 034612 (2004).
[27] A.C. Larsen, *et al.*, Phys. Rev. C **83**, 034315 (2011).